Magnetocaloric effect in the 2D dilute Ising system

Magnetocaloric effect in the 2D dilute Ising system

A V Shadrin[1], V A Ulitko[1] and Y D Panov[1]

[1]Ural Federal University, Ekaterinburg, Russia

E-mail: fynjygame@rambler.ru, vasiliy.ulitko@urfu.ru, yuri.panov@urfu.ru

Abstract. We consider the magnetocaloric effect (MCE) for the 2D Ising system with a fixed concentration of non-magnetic mobile charged impurities. Pseudospin formalism and high-performance Monte Carlo simulations are used to describe the system and, in particular, to obtain the temperature dependences of the MCE parameters for our system. The effect of the impurityimpurity interaction strength on the concentration dependence of the MCE parameters is discussed, as well as the possibility of using the MCE effect to reveal a hidden frustration in the system.

1. Introduction

The magnetocaloric effect (MCE) is the heat absorbed or released as a result of a change in a magnetic field applied to the material. MCE was firstly discovered by Warbourg [1], then the thermodynamic formulation of the principles of adiabatic magnetocaloric cooling was given in [2, 3], followed by the experimental confirmation of adiabatic cooling in [4]. At first, this method was used to reach temperatures below 1 K, but after the discovery of materials exhibiting MCE near room temperature, magnetic cooling became a very active area of research. The most interesting for the researh are compounds with an enhanced, or even giant, MCE, for example $Gd_5(Si_2Ge_2)$ [5], $Mn_{0.96}Cr_{0.04}CoGe$ [6], $DyCrO_4$ and $HoCrO_4$ [7]. MCE is the basis for the creation of environmentally friendly magnetic refrigerators which can be used in everyday life or industry.

Of particular interest is the MCE in frustrated and low-dimensional systems [8, 9, 10, 11, 12, 13]. In the two-dimensional (2D) Ising-type systems, the dependences of the MCE parameters were investigated on magnetovolume coupling for square lattice [14], on the shape and size of geometrically frustrated Ising spin clusters for triangular lattice [15], on a magnitude of spin for honeycomb lattice [16].

In the article we consider the 2D s=1/2 Ising system with a fixed concentration of non-magnetic mobile charged impurities. This dilute Ising model [17, 18] is one of the basic models in the theory of magnetic systems with quenched or annealed disorder, for the binary alloys and in the thermodynamic theory of He^3-He^4 mixtures.

To describe our system we make use of the $S = 1$ pseudospin formalism in which the states for a given lattice site with the pseudospin projections $S_z = \pm 1$ correspond to the two magnetic states with the conventional spin projections $s_z = \pm 1/2$ while the state with $S_z = 0$ corresponds to the charged non-magnetic state. We write the Hamiltonian of the system as follows

$$H = -\tilde{J} \sum_{\langle ij \rangle} S_{zi} S_{zj} + V \sum_{\langle ij \rangle} P_{0i} P_{0j}, \tag{1}$$

where S_{zi} is a z-projection of the on-site pseudospin operator, $P_{0i} = 1 - S_{zi}^2$ is the projection operator on the $S_z = 0$ state, $J = \tilde{J}/s^2$ $(J > 0)$ is the exchange constant, $s = 1/2$, $V > 0$ is the inter-site density-density interaction for impurities, $\langle ij \rangle$ means the nearest neighbors, and the sums run over the sites of a 2D square lattice. The concentration n of charged non-magnetic impurities is fixed: $nN = \sum_i P_{0i} = const$, where N is the number of lattice sites.

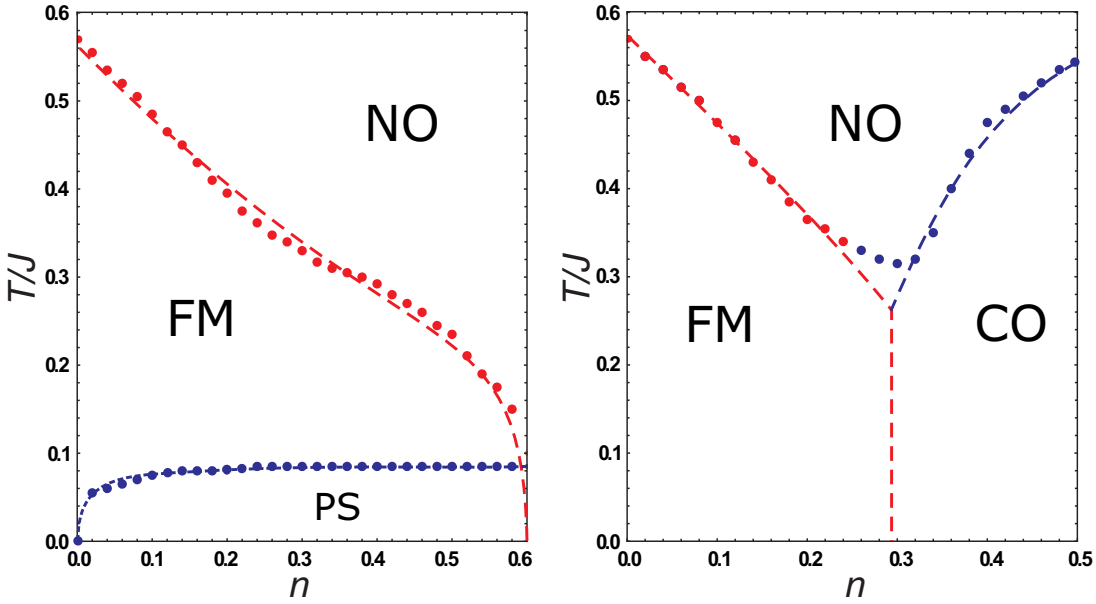

Figure 1. Phase diagrams of a system with the Hamiltonian (1). Left panel: $V/J = 0.1$ (strong exchange case). Right panel: $V/J = 1.0$ (weak exchange case). Circles show the maxima of the specific heat, obtained by the Monte Carlo (MC) simulations. The dashed lines show schematically the boundaries of the non-ordered (NO), ferromagnetic (FM), and charge-ordered (CO) phases, as well as a region with a phase separation (PS).

The system with Hamiltonian (1) demonstrates two types of phase diagrams, their examples are shown in figure1. The left panel in figure1 presents a strong exchange case, $\tilde{J} > V$. In the range of $0 < n < 0.6$, the system reveals two successive phase transitions with lowering the temperature. The first one is related with a ferromagnetic (FM) spin ordering diluted with randomly distributed charged impurities. At low temperatures, the condensation of mobile charged impurities into droplets occurs. This means that the diluted FM phase, in the case of a strong exchange, is unstable with respect to a phase separation (PS) when the FM matrix pushes impurities in order to minimize the associated surface energy. The right panel in figure1 presents a weak exchange case, $\tilde{J} < V$. The FM spin ordering at low n is replaced by the ordering of charged impurities (CO) at moderate n. Hereafter, we restrict ourselves to the range of $0 < n < 0.5$, since for $n > 0.5$ there is no long-range spin ordering with a sufficiently high critical temperature.

The competition of magnetic order and ordering of charged non-magnetic mobile impurities can be realized in systems with a disproportionation or an instability with regard to the charge transfer fluctuations [19], including cuprates. Generally speaking, an increase in the concentration of impurities n suppresses the magnetic order, reduces the critical temperature, and will cause a decrease in the temperature of the maximum value of the MCE parameters, such as the isothermal magnetic entropy change and the adiabatic temperature change. The change in the temperature of the maximum value of the MCE effect with a variation in the chemical composition of the material is well known [20, 21, 22]. But the phase state of the system with

the Hamiltonian (1) depends on the relative value of the spin-spin and the impurity-impurity interactions, as it was demonstrated in similar spin-pseudospin model [23, 24, 25, 26]. The difference in the detailed structure of the system near the critical temperature of the magnetic phase transition should affect the parameters of the MCE, and we study this effect in the present work.

In Sec. 2 we discuss the details of the Monte Carlo (MC) simulations to get the temperature dependences of the MCE parameters for our system, in Sec. 3 we present our results. Short conclusion is presented in last Sec. 4.

2. Calculation of MCE parameters using MC data

The main parameters characterizing MCE are the isothermal magnetic entropy change ΔS_M and the adiabatic temperature change ΔT_{ad} caused by the magnetic field changes. Its visualization is shown in figure 2.

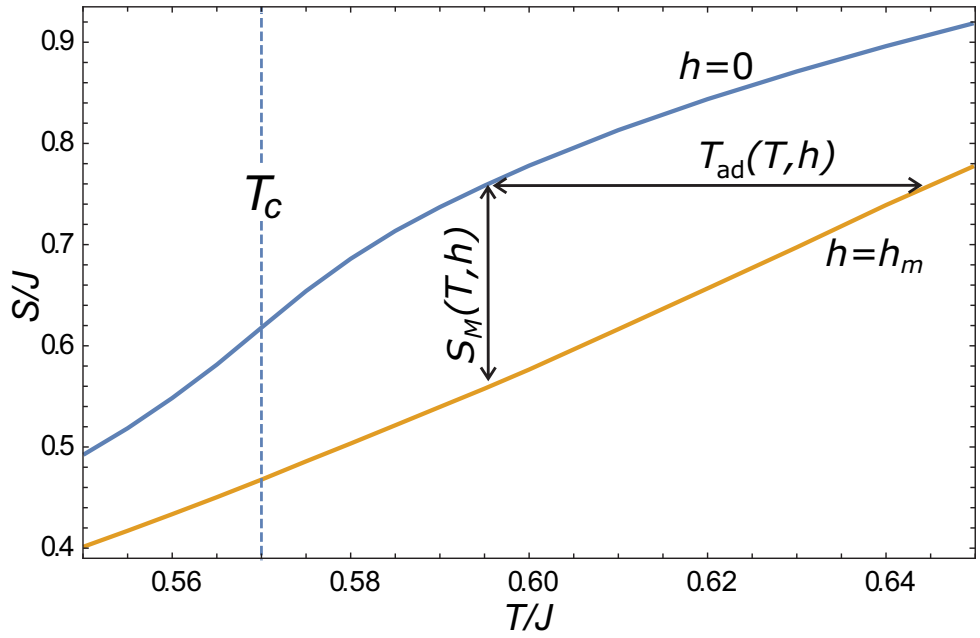

Figure 2. The isothermal magnetic entropy change ΔS_M and the adiabatic temperature change ΔT_{ad}. The dashed line indicates the value of the critical temperature ($n = 0$, $V/J = 0.1$).

The expression for the magnetic entropy change is given by:

$$\Delta S_M(T, h_m) = \int_0^T \frac{C(T', h_m) - C(T', 0)}{T'} dT', \tag{2}$$

where C is the heat capacity. The Maxwell relation $(\partial S/\partial B)_T = (\partial M/\partial T)_B$ gives us another expression for ΔS_M and the equation for ΔT_{ad}:

$$\Delta S_M(T, h_m) = \int_0^{h_m} \left(\frac{\partial M(T, h)}{\partial T}\right)_h dh, \tag{3}$$

$$\Delta T_{ad}(T, h_m) = \int_0^{h_m} \frac{T}{C(T, h)} \left(\frac{\partial M(T, h)}{\partial T}\right)_h dh, \tag{4}$$

where M is the magnetization and h is the external magnetic field.

We use the classical MC simulations to get the temperature dependences of the MCE parameters for a system with Hamiltonian (1) . The Metropolis algorithm was used on a square lattice of 64×64 with periodic boundary conditions. The condition of the constant impurity concentration, $nN = \sum_i P_{0i} = const$, in our program is exactly fulfilled since at each step we change the state of an arbitrarily chosen pair of lattice sites a and b with requiring the conservation of the value $P_{0a} + P_{0b}$.

We implemented high performance parallel computing on the NVIDIA video card, which allowed us to perform calculations for the 64 copies of the system at the same time. For each copy of the system, we reduce the temperature at fixed external magnetic field from the $T_1/J = 1.0$, which is approximately twice larger than the temperature of the magnetic ordering, to the $T_0/J = 0.01$ with the step $\Delta T/J = 0.01$. Then we change the value of the external magnetic field from $h/J = 0$ to $h_m/J = 0.04$ with the step $\Delta h/J = 0.001$. The simulation was done for the impurity concentration from $n = 0$ to $n = 0.5$ with the step $n = 0.1$. For each value of n, T and h we obtain mean values of energy, specific heat C and magnetization M. This allows us to use the discrete approximation for the equations (2–4), the trapezoidal rule for the integrals and the 3-point method for the derivative $\partial M/\partial T$.

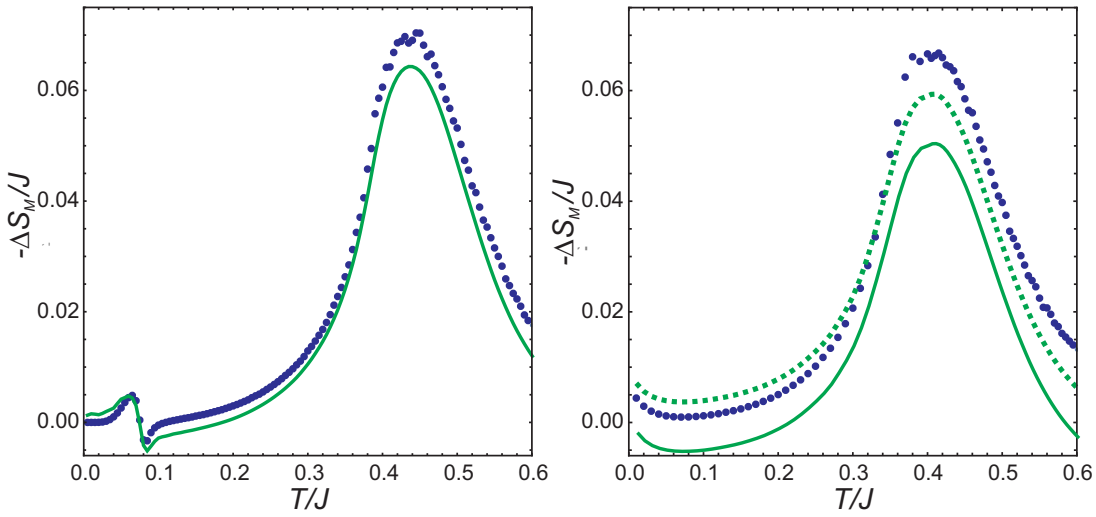

Figure 3. The magnetic entropy change, $n = 0.2$. Left panel: $V/J = 0.1$ (strong exchange case). Right panel: $V/J = 1.0$ (weak exchange case). Solid lines and the circles show the results obtained with equations (2) and (3), respectively. The dotted line shows the result of accounting the contribution (5).

Expressions (2) and (3) enable us to calculate the magnetic entropy change using independent MC data, namely, the specific heat and the magnetization. The results of these calculations agree rather well for the strong exchange case ($\tilde{J} > V$) and differ for the weak exchange case ($\tilde{J} < V$), as shown in figure3 at $n = 0.2$. The possible picture of the ground state configuration for the weak exchange case is shown in figure4.

Unlike strong exchange case, strong interaction of impurities $V > \tilde{J}$ turns into zero the nearest-neighbor impurity correlator and generates the charge ordering at moderate n. As a result, isolated spin clusters are formed surrounded by non-magnetic impurities. These clusters behave as paramagnetic centers and give an additional contribution to the entropy of the system at zero temperature. We make the simplest estimate of this contribution in the form

$$S_0 = N_c \ln 2, \tag{5}$$

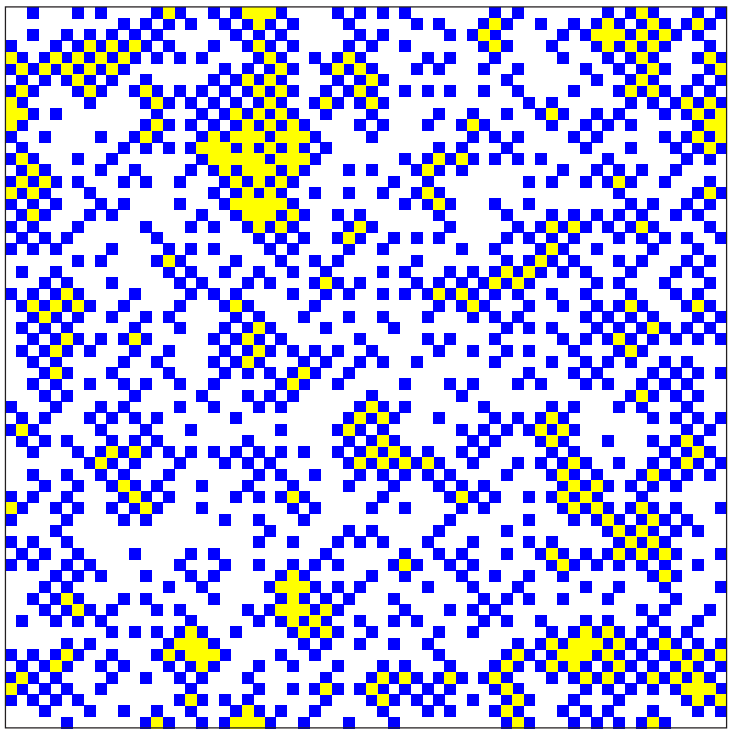

Figure 4. The snapshot of the ground state configuration at $V/J = 1$, $n = 0.3$. White and yellow squares show the lattice sites $S_z = 1$ and $S_z = -1$, respectively. Blue squares show the positions of non-magnetic impurities, $S_z = 0$.

where N_c is the total number of isolated clusters. To find the average numbers for the simplest clusters containing 1, 5 and 8 spins on the 64×64 lattice, we use a program that generates random distributions of charged impurities with the lowest energy. The results are shown in figure5. Accounting for the contribution (5) improves the consistency of the ΔS_M dependencies calculated using (2) and (3), as shown in figure3.

It is worth noting that the difference in the results for ΔS_M calculated using (2) and (3) may indicate some hidden frustrations in the system.

3. Results

From the MC data, we calculated the isothermal magnetic entropy change ΔS_M and the adiabatic temperature change ΔT_{ad} using the discrete approximations for the equations (3) and (4).

Figure 6 and figure 7 show the results for ΔS_M and ΔT_{ad} in the case of strong exchange, $V/J = 0.1$, at $n = 0.0$, 0.1, 0.2, 0.3, 0.4. The temperatures of the maximum values of both parameters approximately follow the change in the critical temperature of magnetic ordering as a function of n. The width of the peaks increases and their height decreases with increasing n due to blurring the FM phase transition by impurities. At low temperatures, there is an additional peak on ΔS_M and ΔT_{ad} dependencies caused by PS transition for the strong exchange case.

Figure 8 and figure 9 show ΔS_M and ΔT_{ad} in the case of weak exchange, $V/J = 1.0$, at $n = 0.0$, 0.1, 0.2, 0.3, 0.4, 0.5. At $n = 0.0$ and $n = 0.1$, these results are very close to the previous ones. But at $n > 0.1$, qualitative differences appear, primarily at low temperatures. The ordering of impurities leads to the appearance of isolated spin clusters. This causes a paramagnetic response, which becomes the maximal one at $n = 0.5$. We obtain $\Delta T_{ad}/J \approx -0.55$ at $T/J = 0.14$.

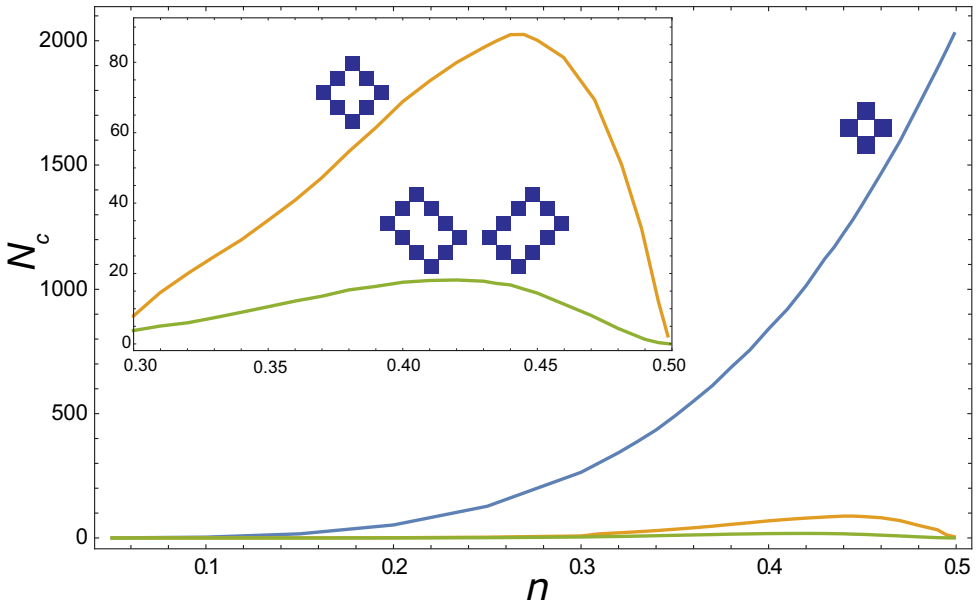

Figure 5. Mean numbers of simplest clusters containing 1, 5 and 8 spins on the 64×64 lattice. An insert shows the results for the clusters containing 5 and 8 spins the lower curves on an enlarged scale.

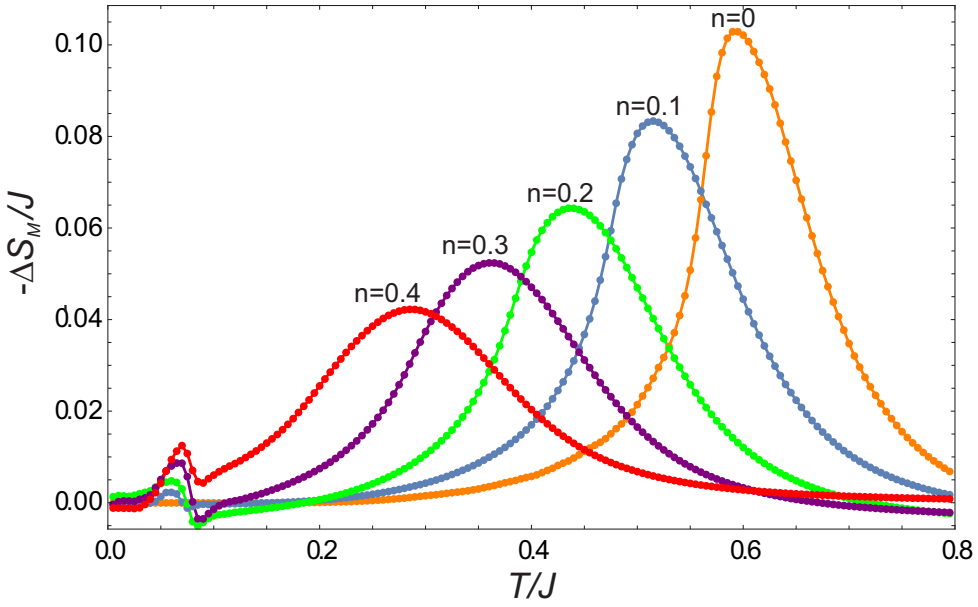

Figure 6. The isothermal magnetic entropy change ΔS_M at $V/J = 0.1$.

The comparison of maximal values of the isothermal magnetic entropy change for the strong and weak exchange cases at $n = 0.0, 0.1, 0.2, 0.3, 0.4$ is shown in figure 10. As mentioned above, the results for $n = 0.0$ and $n = 0.1$ are similar, but with moderate n, the maximum value of ΔS_M for the weak exchange case becomes lower due to the more efficient disordering of FM state by charged mobile impurities.

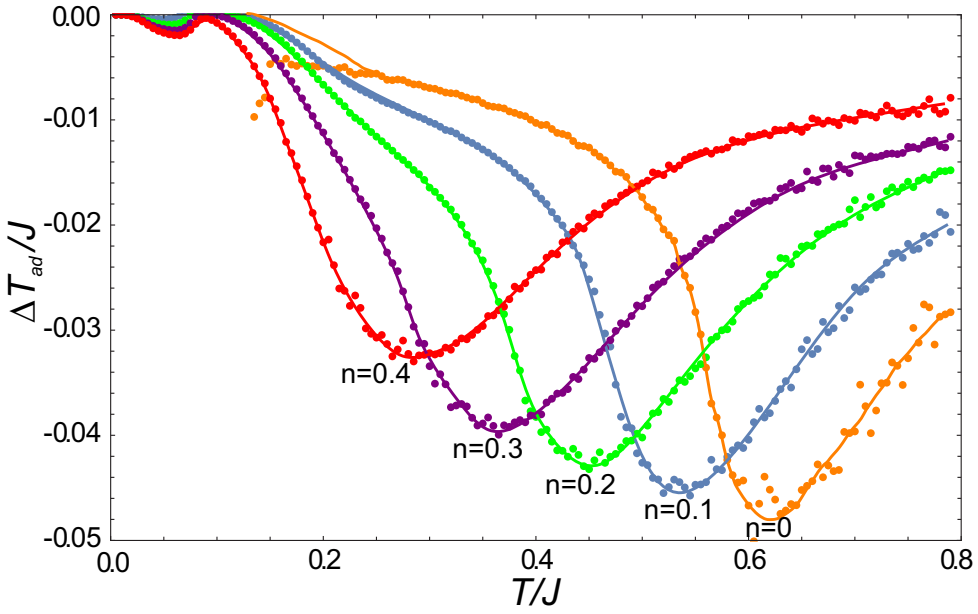

Figure 7. The adiabatic temperature change ΔT_{ad} at $V/J = 0.1$.

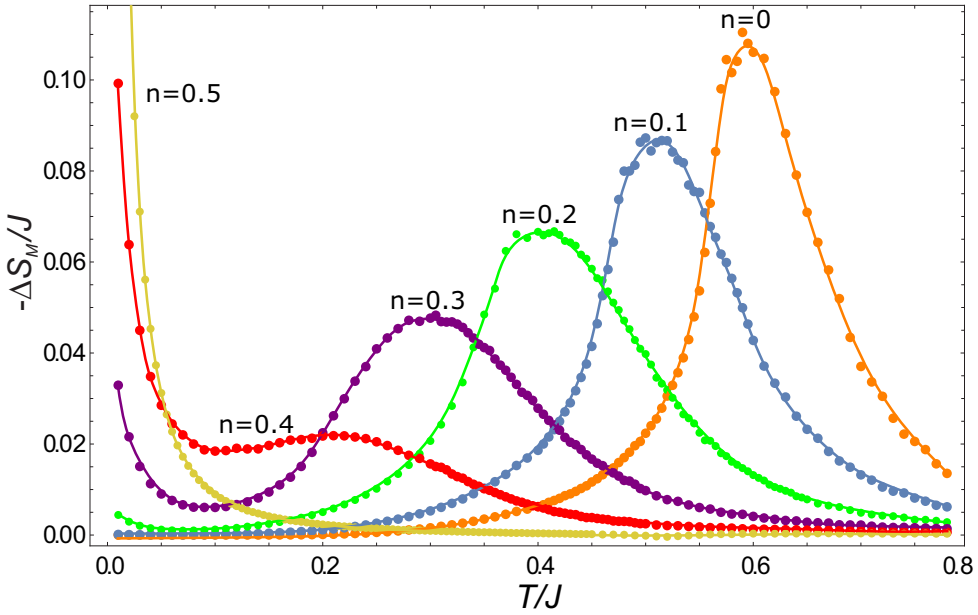

Figure 8. The isothermal magnetic entropy change ΔS_M at $V/J = 1.0$.

4. Conclusion

We considered MCE for the 2D dilute Ising system with a fixed concentration of non-magnetic mobile charged impurities, which is one of the basic models in the theory of magnetic systems with quenched or annealed disorder. Using the classical Monte Carlo simulations, we found that the temperatures of the maximum MCE parameters decrease with increasing concentration of non-magnetic impurities. At low temperatures, an additional enhancement of MCE occurs, caused by the PS transition in the case of strong exchange, while in the weak exchange case, the ordering of impurities leads to the paramagnetic nature of MCE. Also, the possibility to reveal

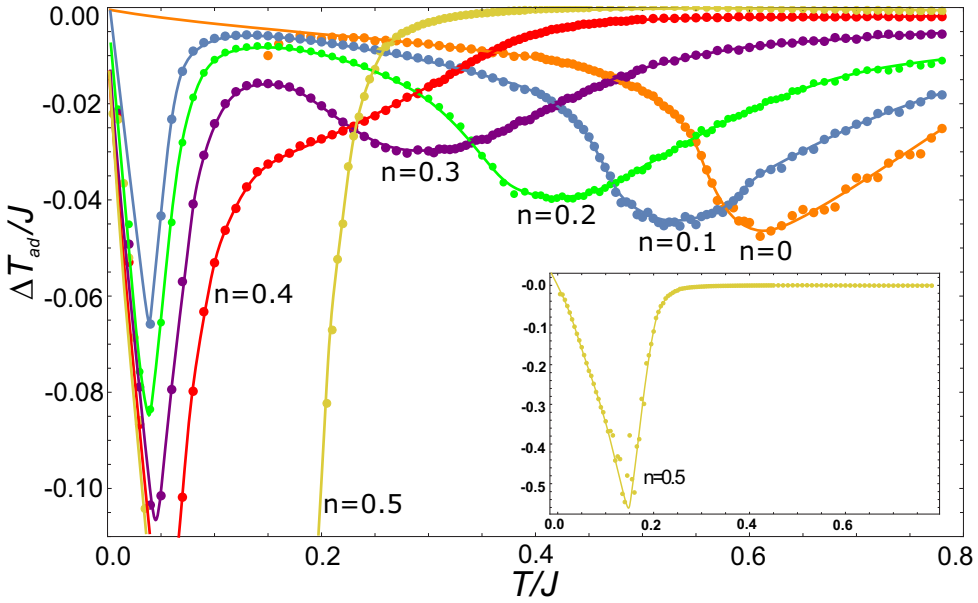

Figure 9. The adiabatic temperature change ΔT_{ad} at $V/J = 1.0$. An insert shows separately the results for $n = 0.5$.

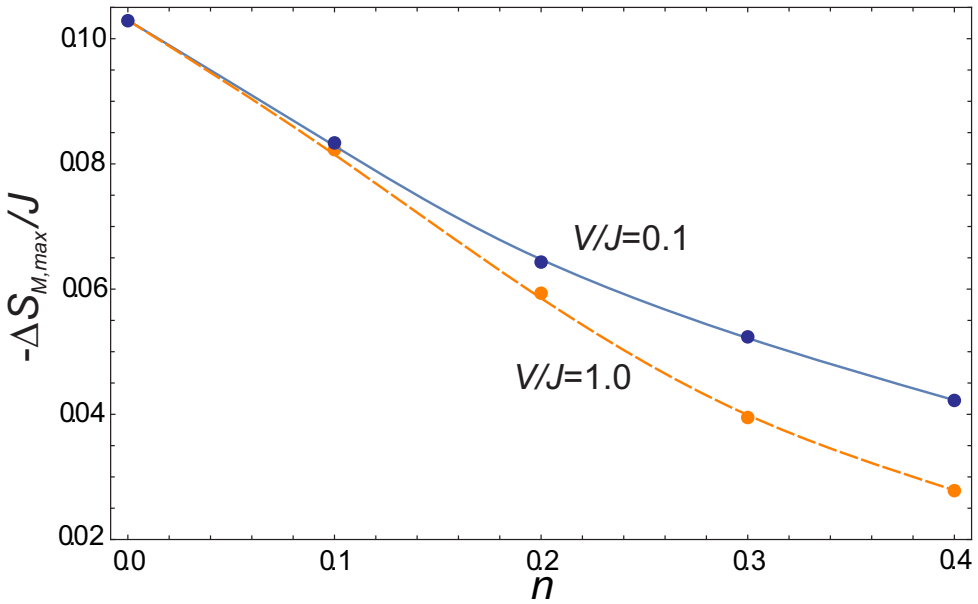

Figure 10. The comparison of maximal values of the isothermal magnetic entropy change for the strong and weak exchange cases.

a hidden frustration in the system using the MCE data was predicted.

Acknowledgement
This work was supported by Program 211 of the Government of the Russian Federation (Agreement 02.A03.21.0006), the Ministry of Education and Science of the Russian Federation (projects nos. 2277 and 5719).

References

[1] Warburg E 1881 *Annalen der Physik* **249** 141
[2] Debye P 1926 *Annalen der Physik* **386** 1154
[3] Giauque W F 1927 *J. Am. Chem. Soc.* **49** 1864
[4] Giauque W F and MacDougall D P 1933 *Phys. Rev.* **43** 768
[5] Pecharsky V K and Gschneidner Jr K A 1997 *Phys. Rev. Lett.* **78** 4494
[6] Trung N T, Biharie V, Zhang L, Caron L, Buschow K H J and Brck E 2010 *Appl. Phys. Lett.* **96** 162507
[7] Midya A, Khan N, Bhoi D and Mandal P 2013 *Appl. Phys. Lett.* **103** 092402
[8] Zhitomirsky M E 2003 *Phys. Rev. B* **67** 104421
[9] Zhitomirsky M E and Honecker A 2004 *J. Stat. Mech.: Theory Exp.* **2004** P07012
[10] Honecker A and Wessel S 2006 *Physica B* **378-380** 1098
[11] Schmidt B, Thalmeier P and Shannon N 2007 *Phys. Rev. B* **76** 125113
[12] Trippe C, Honecker A, Klümper A and Ohanyan V 2010 *Phys. Rev. B* **81** 054402
[13] Lambert C, El Hadri M, Hamedoun M, Benyoussef A, Mounkachi O and Mangin S 2017 *J. Magn. Magn. Mat.* **443** 1
[14] Amaral J S, Goncalves J N and Amaral V S 2014 *IEEE Trans. Magn.* **50** 1
[15] Žukovič M 2015 *J. Magn. Magn. Mat.* **374** 22
[16] Aknc Ü, Yüksel Y and Vatansever E 2018 *Phys. Lett. A* **382** 3238
[17] Rys F 1969 *Helv. Phys. Acta* **42** 606
[18] Blume M, Emery V J and Griffiths R B 1971 *Phys. Rev. A* **4** 1071
[19] Moskvin A S 2013 *J. Phys.: Condens. Matter* **25** 085601
[20] Shen B G, Sun J R, Hu F X, Zhang H W and Cheng Z H 2009 *Adv. Mater.* **21** 4545
[21] Inishev A A, Gerasimov E G, Mushnikov N V, Terent'ev P B and Gaviko V S 2018 *Physics of Metals and Metallography* **119** 1036
[22] Zhang H, Gimaev R, Kovalev B, Kamilov K, Zverev V and Tishin A 2019 *Physica B* **558** 65
[23] Panov Y D, Moskvin A S, Chikov A A and Avvakumov I L 2016 *J. Low Temp. Phys.* **185** 409
[24] Panov Y D, Moskvin A S, Chikov A A and Avvakumov I L 2016 *Journal of Superconductivity and Novel Magnetism* **29** 1077
[25] Panov Y D, Budrin K S, Chikov A A and Moskvin A S 2017 *JETP Letters* **106** 440
[26] Panov Y, Ulitko V, Budrin K, Chikov A and Moskvin A 2019 *J. Magn. Magn. Mat.* **477** 162